

MEASUREMENT OF LOSS OF DT FUSION
PRODUCTS USING SCINTILLATOR DETECTORS IN
TFTR

BY

D.S. DARROW, H.W. HERRMANN, D.W. JOHNSON, ET AL.

Presented at the Tenth Topical Conference on
High Temperature Plasma Diagnostics
Rochester, NY, 8-12 May, 1994

Work supported by US DoE Contract DE-AC02-76CH0-3073

Princeton University
Plasma Physics Laboratory

MASTER

DISTRIBUTION OF THIS DOCUMENT IS UNLIMITED



DISCLAIMER

This report was prepared as an account of work sponsored by an agency of the United States Government. Neither the United States Government nor any agency thereof, nor any of their employees, make any warranty, express or implied, or assumes any legal liability or responsibility for the accuracy, completeness, or usefulness of any information, apparatus, product, or process disclosed, or represents that its use would not infringe privately owned rights. Reference herein to any specific commercial product, process, or service by trade name, trademark, manufacturer, or otherwise does not necessarily constitute or imply its endorsement, recommendation, or favoring by the United States Government or any agency thereof. The views and opinions of authors expressed herein do not necessarily state or reflect those of the United States Government or any agency thereof.

DISCLAIMER

Portions of this document may be illegible in electronic image products. Images are produced from the best available original document.

Measurement of Loss of DT Fusion Products Using Scintillator Detectors in TFTR

D. S. Darrow, H. W. Herrmann, D. W. Johnson, R. J. Marsala, R. W. Palladino,
and S. J. Zweben,

Princeton University, Plasma Physics Laboratory, PO Box 451, Princeton, NJ 08543

M. Tuszewski,

Los Alamos National Laboratory, Los Alamos, NM 87545

Abstract

A poloidal array of MeV ion loss probes previously used to measure DD fusion product loss has been upgraded to measure the loss of alpha particles from DT plasmas in TFTR. The following improvements to the system have been made in preparation for the use of tritium in TFTR: (1) relocation of detectors to a neutron-shielded enclosure in the basement to reduce neutron-induced background signals; (2) replacement of ZnS:Cu (P31) scintillators in the probes with the $Y_3Al_5O_{12}:Ce$ (P46) variety to minimize damage and assure linearity at the fluxes anticipated from DT plasmas; and (3) shielding of the fiber optic bundles which carry the light from the probes to the detectors to reduce neutron- and gamma-induced light within them. In addition to the above preparations, the probes have been absolutely calibrated for alpha particles by using the Van de Graaf accelerator at Los Alamos National Laboratory. Alpha particle losses from DT plasmas have been observed, and losses at the detector 90° below the midplane are consistent with first orbit loss.

I. Introduction

Production of DT plasmas in TFTR has begun. Some of the aims of the DT program are the measurement of alpha particle confinement, the investigation of collective alpha instabilities, a search for alpha heating, and the development of alpha particle diagnostics. These topics all are relevant to ITER and subsequent machines. Of particular importance to the design of ITER is the loss rate of alpha particles to the walls. A loss rate of more than a few percent of the production rate would cause damage to the first wall. Therefore, it is useful to measure the losses of alpha particles from TFTR DT plasmas and to understand how those losses should scale to ITER.

This paper describes the escaping alpha particle diagnostic on TFTR,^{1,2} concentrating on modifications made to prepare the diagnostic for use in DT plasmas. Section II describes the probes and detectors and how they were prepared for DT operation, Section III describes the choice and characteristics of new scintillators chosen for the DT campaign, Section IV describes shielding of the detectors from neutron and gamma radiation. Section V describes efforts to minimize radiation-induced light in the optical fiber bundles, Section VI describes the method of calibrating the probes, and Section VII describes the data analysis procedure and some initial DT results.

II. Probes and Detectors

Fig. 1 shows the schematic layout of the TFTR escaping alpha diagnostic. There are four probes inside the vacuum vessel just outside the limiter radius which detect escaping charged fusion products and other fast ions. The probes and their protective graphite heat shields³ are shown in Fig. 2. The probes are located at 90°, 60°, 45°, and 20° below the outer midplane in TFTR, and the magnetic fields are configured such that the ion grad-B drift is always downward, toward these probes. Figure 3 displays the principle of operation of the probes: large gyroradius ions which pass through the two collimating apertures of the probe are dispersed onto the planar scintillator according to their gyroradius and pitch angle. The image of the light produced by the impact of the ions in the scintillator is carried, via lenses and a coherent fiber optic bundle, to detectors in the TFTR Test Cell Basement. The detectors include intensified videocameras and photomultiplier tubes which measure both the spatial pattern of the light, and the total light from each probe. The detectors do not count pulses but measure the intensity of the light produced, since a high power DD shot results in $\sim 10^8$ particles per second to each detector.

A quartz plate bearing the inorganic scintillator (see Section III below) mounts at the end of each probe tube, and is covered by a tantalum end cap, which reduces the flux of X-rays to the scintillator. The scintillator holder is electrically isolated from the vessel, and its temperature is measured by a thermocouple. The 90°, 60°, and 45° probes are fixed in position with their apertures ~1.2 cm further out in minor radius than the limiter. The limiter surface is essentially a circle centered on the midplane at $R=2.606$ m, with a radius of 0.99 m. The 90° and 60° probes have one lens within their probe stems to relay the image of the scintillator to the fiber bundle outside the vacuum. The 45° detector has three lenses to relay the image, since its probe shaft is longer. The 20° ("midplane") probe⁴⁻⁶ contains two internal lenses and a fiber optic bundle inside the probe shaft to transmit the image of the scintillator to the vacuum window.

Outside the vacuum window of each probe, is mounted a 50×50 coherent quartz fiber optic bundle measuring $1.2 \text{ cm} \times 1.2 \text{ cm}$. These bundles pass through the Test Cell floor directly under the machine, with the minimum possible length of fiber exposed to the neutron flux near the tokamak. Even with only ~1.5 m exposed, there was still significant neutron-induced background light in the fiber during DD plasmas, and shielding was placed around it before the DT campaign (see Section V). The fibers are routed through the 2 m thick floor, and travel 6 m further down, into a neutron-shielded enclosure at the Test Cell Basement floor level where the detectors are located (see Section IV).

The detectors are mounted on a $91 \text{ cm} \times 91 \text{ cm}$ optical table inside a light tight box within the neutron shielding enclosure. All detectors in this system contain interference filters, which pass only a band of wavelengths centered at 550 nm, with a FWHM of 70 nm. This passband corresponds roughly to the scintillator emission curve, although the latter has maximum intensity at 535 nm. Figure 4 depicts the detector layout. The four fiber optic bundles from the four probes in the vessel are clamped together in a mount at the left side of the box. Two ITT F4577 intensified videocameras view the four fiber bundles by beamsplitters. The leftmost beamsplitter reflects 40% of the light incident on it to the main camera. The second beamsplitter reflects about 5% into the secondary camera, which is usually adjusted to capture signals that would otherwise be too bright on the main camera. The second camera also serves as a backup in case the main camera should fail during a campaign. The gain voltage and the gate pulse duration for the microchannel plate intensifier in each camera can be controlled from the TFTR Control Room through the CICADA computer system and associated CAMAC modules in the Test Cell Basement.

The video signals from the cameras are transmitted directly to the Control Room through fiberoptic links. In the Control Room, the video signals from the cameras are taped and digitized.

Beyond the two beamsplitters for the camera is an $f/2$ focusing lens, which images the ends of the fiber optic bundles, through a beamsplitter, onto four photomultiplier tubes. These are referred to as "waveform photomultipliers" since their outputs are recorded in the TFTR waveform database. Each tube receives light from one bundle. Ideally, if the only light in the fiber bundles came from fusion products striking the scintillator, these photomultiplier signals would correspond to the rate of fusion product loss to each probe. In practice, there is significant neutron and gamma-induced background light in the fibers, plus some signal in the photomultipliers due to the neutron and gamma flux within the detector enclosure, ~10% of the total. The detector enclosure is in a location well shielded against neutrons and gammas already, and there is little free space around the tubes themselves, so the second noise level is irreducible. To diminish the amount of signal coming from background light in the fiber bundles, opaque masks have been positioned so that light coming only from areas of the scintillator which can be struck by fast ions is admitted to the photomultipliers. Even with this masking, the fraction of the photomultiplier signal which is due to fusion products is usually only 25 to 35% for high current discharges. The photomultiplier system can still provide very useful results on fluctuations in the loss. In addition, measurement of ICRF tail ion loss, which can be performed in plasmas with very low neutron rates, is easily done with these photomultipliers without any need for background subtraction. The signals are simultaneously recorded at two gains by both fast (usually 100 kHz) and slow (usually 5 kHz) digitizers, and are plotted in the control room after each shot. These signals provide a convenient means for cursory examination of a shot.

The $f/2$ lens also focuses light onto a set of two plastic fiber optic bundles. This set can be moved by command from the Control Room to intercept the image of one or another pair of detectors: either the 90° and the 20° , or the 60° and 45° units. These fibers and their positioner appear at the extreme right of Fig. 4. Each of these plastic fiber bundles is comprised of 50 fiber optic ribbon cables, laid side by side, and those 50 ribbons split the light between ten photomultiplier tubes. These signals are then able to give a rough profile of the loss versus pitch angle, and can record changes that occur at higher frequencies than the videocamera can detect, up to 2.5 kHz. These detectors are intended to resolve changes in the pitch angle distribution of the loss due to MHD events. They do, however, suffer from low signal to noise ratios, since the light is divided between ten photomultipliers.

Directly adjacent to the four fiber bundles coming from the tokamak are the ends of four single plastic optical fibers, which carry light from an LED. These four lights are also viewed by the cameras, and can be used to check for time-variations of the camera response during a shot. With the present ITT cameras, such variations are quite small.

Immediately in front of the four fiber bundles is a moveable rack which contains several neutral density filters and a white plate. The neutral density filters are arranged in three combinations useful under various TFTR operation conditions. In these conditions, the signal from one or two of these probes is much larger than that from the others. The filters allow various combinations of the probes to be attenuated by factors of 10 or 100, so that the signal from the dimmer probes can be seen simultaneously. The white plate is used for calibrations of the camera responses, when illuminated by the calibration lamp (see below).

Just above the cameras is an Oriel 20 W quartz-halogen lamp used for calibrations. It serves, in conjunction with the white plate, for white field calibration of the cameras and photomultipliers. It also can be used to illuminate the ends of the fiber bundles to verify their position periodically in the field of view of the cameras. Also used for calibration is a green LED which is situated above the photomultipliers. This LED can be powered with a square wave of controllable amplitude, providing a convenient calibration and functionality test for all of the photomultipliers.

The signals from the two cameras, as noted above, are transmitted to the Control Room, and recorded on VHS format videotape. The images are also captured by a video frame grabber in an IBM PC compatible computer, one computer for each camera, and displayed on video monitors. The frame grabbers are triggered by the CICADA computer, and digitize up to 42 frames of data. After each shot, the data from the regions of the camera images which correspond to the fiber optic bundles is compressed and stored on a hard disk. The data capture software also allows review on the video monitor of the most recent shot, and some rudimentary analyses. It transfers data between shots to PPPL's centralized VAX computers for more detailed analysis and archival storage.

III. Scintillators for DT Operation

All of the probes in the TFTR escaping alpha diagnostic use scintillators comprised of powdered inorganic phosphors deposited onto quartz plates 2.5×2.5 cm. During the 1992

campaign, that phosphor was ZnS:Cu (P31). This material is bright, emits at 530 nm, does not lose luminosity until well above 100° C, and is commonly used in oscilloscope display tubes. However, testing of P31 with alpha particles at the Los Alamos National Laboratory Van de Graaf accelerator indicated that its response would saturate at fluxes below or at those anticipated from DT plasmas,⁷ about $10^{10} \alpha \text{ cm}^{-2} \text{ sec}^{-1}$. The same tests indicated that its response would diminish significantly with alpha particle fluence. For these reasons, an alternate phosphor was sought.

Several candidate scintillator materials were chosen from specifications for possible replacements for P31. These were: Y₃Al₅O₁₂:Ce (P46), YVO₄:[V]:Dy (GTE Sylvania Corporation⁸ designator 2370), and Y₃(Al,Ga)₅O₁₂:Ce (Imaging & Sensing Technology Corporation^{9,10} designator PX87). The criteria for evaluation of these scintillator materials were that their response to alpha particles be linear beyond the expected range of alpha particle flux, that the anticipated fluences would not cause significant loss of brightness (damage to the scintillator material), that the light decay after excitation in 10 μsec or less, that the emitted light be in the wavelength band of maximum sensitivity of the videocameras and photomultipliers (420 to 600 nm), and that the emission not be reduced by temperatures up to 100° C.

All of the scintillators chosen for testing satisfied the emission wavelength requirement. The temperature response of the scintillators was measured by placing them on a hot plate and exposing them to 4.5 MeV alpha particles from a ²⁴⁴Cm source.¹¹ This test showed that the response of PX87 declines rapidly above 70° C, making it an undesirable choice. The manufacturer's specification indicated that the 2370 phosphor response to ultraviolet light increases slightly with temperature, up to 250° C. A similar variation in luminosity under bombardment by α particles was assumed. The response of P46 diminishes above 120° C, falling linearly to 15% at 300°C.

The linearity, time response, and effect of fluence upon brightness were evaluated for the P46 and 2370 at the LANL Van de Graaf accelerator.¹² The 2370 phosphor was found to have too long a time constant, ~30 μsec. In contrast, P46 has a very short time constant, ~0.16 μsec,^{10,12} was linear far above the range anticipated for DT alpha flux, and proved to be extremely resistant to damage. The major drawback of P46 is that it is, for 3.5 MeV alpha particles, approximately 30 times less luminous than P31. This lower luminosity had later repercussions in the signal-to-noise ratio, given the intensity of neutron-induced light in the fiber optics (see Section V).

The scintillators for the DT campaign were fabricated by the Imaging & Sensing Technology Corporation⁹ using the P46 phosphor. The quartz plate was first coated with 200 nm thick layer of aluminum before coating with P46. The aluminum coating aids in dissipating the accumulated charge on the scintillator, and also serves to reflect emitted light back toward the detection optics. The P46 coating was deposited as a powder with average grain size of a few microns. The total thickness was 1.7 mg/cm², which is just enough to stop 3.5 MeV alpha particles when incident at 70° from the normal. This thickness was chosen in order to minimize the light produced by neutrons and gamma rays in the scintillator. Results from DT shots show that only at the very highest neutron rates obtained to date (2×10^{18} n/s) is there any background light from neutrons and gammas striking the scintillator visible above that produced by the optical fibers. The phosphor thickness is not sufficient to fully stop the DD fusion products, 1 MeV tritons and 3 MeV protons, reducing the detection efficiency for these particles somewhat.

IV. Detector Shielding

From 1988 to 1992, only one camera and a few photomultipliers were used to measure the light from these probes. These detectors were located in a box without radiation shielding 1 m below the ceiling of the Test Cell Basement. A small but noticeable amount of radiation-induced noise could be seen in the videocamera images during high power DD shots. This noise was enough that increasing it by 100 times by going to DT plasmas would have had a serious effect upon the quality of the data. In addition, about 25% of the signal from the photomultiplier tubes at that location was determined to be from neutrons and gamma rays striking in the tubes. Multiplication of this noise by a factor of 100, while reducing the actual signal level due to the change to P46 scintillators, meant that the photomultipliers would produce no useful data during DT operation.

Given these projections of what would happen if the detectors remained in the same location, the possibility of shielding was considered. Measurements of the neutron flux at the detector location and in a nearby pre-existing radiation shielding enclosure showed that the flux of gammas and neutrons could be reduced by a factor of 30 to 100 by moving the detectors into that enclosure. That would assure that the detectors still provided useful data, and the enclosure was sufficiently close that the existing fiber optic bundles could reach it.

In preparation for the DT campaign, the detectors were moved to this radiation enclosure, which has walls comprised of 40 cm of borated polyethylene and 20 cm of lead. In the process of this move, a second videocamera and the plastic fiber bundle/photomultiplier array were added. As cables into the enclosure were installed, care was taken to avoid line-of-sight streaming paths from the area directly beneath the tokamak to the interior of this enclosure. During the same time interval, many unused holes in the Test Cell floor were plugged to reduce the neutron flux in the basement.

Videocamera data from the highest neutron rate shots to date shows no evidence of neutron or gamma ray induced noise produced within the camera. The level of radiation-induced background within the photomultipliers is ~10% of the total signal. Given that the total signal level is much reduced, this fraction represents a much smaller absolute background. The largest contribution to the background is light generated within the quartz fiber optic bundles by neutrons and gamma rays.¹³ (See Section V below)

V. Shielding of the Fiber Optic Bundles

No background light from the quartz fiber bundles had previously been observed. However, from the first few days of DD plasmas in July 1993, it became apparent that, by switching to P46, the scintillator signal had diminished to the point that the neutron and gamma background was comparable in magnitude to it. Given that the background light from 14 MeV DT neutrons would probably be higher, per neutron, than for the 2.5 MeV neutrons, thus further reducing the signal to background ratio, it was decided that shielding of the fiber optic bundles near the tokamak was required. Later, the ratio of background light per neutron at 14 MeV versus at 2.5 MeV was measured to be 1.5 ± 0.2 .

The shielding for the fiber optic bundles needed to be self-supporting, compact, and fireproof. In addition, since it physically adjoined the toroidal and poloidal field coils, it could not contain large pieces of conducting material, such as lead, as these would experience large eddy current forces during disruptions. Furthermore, the shielding had to be constructed such that it could be installed by one person working in very tight quarters, as the area where the fiber bundles run from the vessel to the floor is only 1.5 m high and 1 m at its widest. The design depicted in Fig. 5 was developed to satisfy all these constraints.

The shielding was built using semicircular blocks fabricated for this purpose. The blocks were molded from lead shot and granules of boron frit, bonded by an epoxy. The use of

lead shot in an insulating matrix provided the high gamma shielding power of the lead, while greatly reducing the eddy current forces that a solid lead brick of the same size would experience. The hydrogen in the epoxy and the boron frit permitted thermalization and absorption of the neutrons. The top and bottom of each cast block contained interlocking grooves so that, when stacked, they did not slide with respect to one another. The blocks were assembled into two upright cylinders running from the floor under the tokamak to within 20 cm of the vessel, with the fiber optic bundles running up the center of each. Where the fiber optic bundles ran along the floor, the blocks were stacked to form a tunnel through which the bundles could pass, as seen in Fig. 5. Additional borated polyethylene blocks were added to the sides and top of the structure, and the whole assembly was wrapped in Nomex cloth to fireproof it.

Benchmark tests with a PuBe neutron source and theoretical calculations indicated that the neutron flux incident from the side of the shielding blocks would be attenuated by about a factor of seven to ten. However, measurements of the background light produced by DD plasmas both before and after the shielding installation showed that the light produced in the fibers was reduced by about a factor of two. Streaming of neutrons down the center of the shielding and the lack of shielding around the first 20 cm of fiber probably account for the remaining radiation-induced light.

VI. Absolute Calibration of the System

The detector system, in its past configuration, had been calibrated for DD fusion products.¹⁴ The new arrangement has now been absolutely calibrated for fluxes of 3.5 MeV alpha particles.

The calibration is used to establish the absolute sensitivity of the main videocamera in the system. Other detectors can then be cross-calibrated to that camera. It depends upon a mobile extended light source, which is filtered to emit only in the passband of the detector system. At a specific brightness (current) setting, this source was set in the place of the scintillator of each probe. The main camera recorded the brightness at a designated gain and gate duration.

The same light source arrangement was then taken to the Los Alamos National Laboratory Van de Graaf accelerator facility. A beam of 3.5 MeV alpha particles of a known current was directed onto a P46 scintillator identical to the ones in TFTR, at the same angle of

incidence. The resulting light was measured by a photomultiplier tube. Then, the illuminated surface of the light source was masked to an area comparable to the spot size of the alpha particles on the scintillator. With the light source positioned at the same distance and angle from the photomultiplier as the scintillator, and set at the same brightness as was used in the TFTR vacuum vessel, the photomultiplier output was recorded.

The absolute response of the camera at the gain used for the in-vessel calibration is then given by:

$$R = (F_E \Gamma_{VdG} V_\alpha T_{gate}) / (A V_{Is} B_{Is})$$

Here, Γ_{VdG} is the number of 3.5 MeV alpha particles per second striking the scintillator in the Van de Graaf setup, V_α is the voltage output of the photomultiplier due to alpha particles striking the scintillator in the Van de Graaf setup, V_{Is} is the voltage output of the photomultiplier due to the light source when masked and placed in the Van de Graaf setup, A is the luminous area, in cm^2 , of the light source in the Van de Graaf setup when masked, B_{Is} is the video digitizer output, in counts, of the intensity measured by the camera when the light source replaced the scintillator on a given probe inside the vacuum vessel, and T_{gate} is the gate width (exposure time) in milliseconds of the camera during the in-vessel calibration with the light source. F_E is a factor which arises because the tests on the Van de Graaf were performed with 3.5 MeV alpha particles, while the alphas that reach the scintillator in some probes have passed through a 3 μm thick aluminum foil in the aperture of the probe which reduces their energy to 2.7 MeV. That reduction in energy causes a single alpha to produce less light in those probes in the TFTR vessel than an alpha accelerated by the Van de Graaf. $F_E = 1.3$ for the 90°, 60°, and 45° probes, which have the 3 μm foil, and $F_E = 1$ for the 20° probe, which has no foil. The response, R , is in units of $\alpha \text{ cm}^{-2} \text{ sec}^{-1} (\text{digitizer count} / \text{msec})^{-1}$. The R factors for each probe vary due to differences in the optics in each. They are listed in Table 1.

The principal uncertainties in the calibration are: the luminosity of the scintillator when exposed to a given 3.5 MeV alpha particle flux ($\pm 50\%$), the repeatability of the output of the calibration light source ($\pm 25\%$), and variation of the particles' angle of incidence upon the scintillator ($\pm 15\%$). Together, these yield about a 60% uncertainty in the absolute calibration.

Changes in the absolute response can occur due to a wide variety of factors, including the camera sensitivity, the transmission of the quartz fiber bundles, vacuum window, and lenses, and the response of the scintillator to alphas. Of these, the only one which can be measured with some confidence is the camera response. This is done by utilizing the calibration lamp and the white plate to take daily checks of the camera sensitivity. Over several months of the DT run, this check shows the camera sensitivity varying $\pm 6\%$ on a day-to-day basis, but with no long term trend. The optical fibers, lenses, and windows may be progressively darkening due to their exposure to DT neutrons. Also, due to release of some organic materials into the TFTR vacuum vessel in 1992, there is some residue on the vacuum windows and lenses of the probes whose opacity may be changing with time.

The absolute response of the probes was compared with a code which simulates the fusion source rate of the plasma, the orbits of the fusion products, and the detector geometries. This calculation is subject to uncertainties in the probe aperture size and acceptance ($\pm 20\%$) and in the neutron rate ($\pm 7\%$), and variations in the modeled fusion reaction rate and current profiles ($\pm 10\%$). For 0.6 MA shots, the model predicts a signal in the 90° probe about 1.6 times the observed signal, a difference which is within the uncertainties.

VII. DT Results

During a plasma shot, 42 videocamera images are captured by a frame grabber in an IBM PC compatible computer. Thereafter, they are compressed and transferred to the central VAX computer system. There, the data can be analyzed to determine the time history and magnitude of the losses, as well as the pitch angle and gyroradius distributions. Fig. 6 depicts raw data from the 90° probe, averaged over the last 0.3 sec of neutral beam injection of shot 73268, which is the shot which has produced the highest DT neutron rate as of this writing.¹⁵ The black level of the camera, the neutron background, and the alpha particle signal are all clearly visible in this plot. A detailed analysis of this data indicates that the loss is of alpha particles at their birth energy, and at a pitch angle which corresponds to first orbit loss.¹⁶ Likewise, the absolute magnitude of the loss agrees with computer simulations of the discharge.

Summary

The escaping alpha diagnostic on TFTR has been modified in preparation for the DT campaign. Modifications include: relocation of the detectors to a neutron shielded enclosure

in the TFTR Test Cell Basement, addition of a second camera to the detector system, replacement of the scintillators within the probes by P46, and rerouting and shielding of the fiber optic bundles near the tokamak to minimize their exposure to neutron and gamma radiation, thereby reducing background light produced in the fibers. In addition, an absolute calibration of the probes for 3.5 MeV alpha particles has been obtained.

Data has been taken with this diagnostic during the initial DT shots on TFTR. Alpha particle losses have been observed in all of the probes. The losses to the 90° detector are consistent with first orbit loss, ie no anomalous losses need be postulated.

Acknowledgements

The authors wish to thank K. Hill, L. P. Ku, G. Lemunyan, A. L. Roquemore, and M. Vocaturo, for their assistance with preparations for DT operations, and R. Hawryluk, K. McGuire, J. Strachan, and K. Young for their support of this diagnostic effort. Thanks are also due M. Diesso for development of the analysis software for this data. This work was supported by US DoE contract number DE-AC02-76-CHO-3073.

References

- ¹S. J. Zweben, *Rev. Sci. Instrum.* **60**, 576 (1989).
- ²S. J. Zweben, R. Boivin, S. L. Liew, D. K. Owens, J. D. Strachan, and M. Ulrickson, *Rev. Sci. Instrum.* **61**, 3505 (1990).
- ³S. J. Zweben, R. Boivin, D. Darrow, D. Loesser, S. S. Medley, M. McSmith, D. K. Owens, and M. Ulrickson, *Rev. Sci. Instrum.* **63**, 4565-4567 (1992).
- ⁴R. L. Boivin, S. Kilpatrick, D. Manos, and S. J. Zweben, *Rev. Sci. Instrum.* **61**, 3208 (1990).
- ⁵R. L. Boivin, Ph.D. Thesis, Princeton University, 1991.
- ⁶D. S. Darrow, R. L. Boivin, and S. J. Zweben, *Rev. Sci. Instrum.* **63**, 4562-4564 (1992).
- ⁷M. Tuszewski and S. J. Zweben, *Rev. Sci. Instrum.* **63**, 4542 (1992).
- ⁸GTE Sylvania Corporation, Towanda, PA
- ⁹Imaging and Sensing Technology Corporation, Horseheads, NY
- ¹⁰"Phosphor Resource Manual for Industrial and Military Cathode Ray Tubes," Imaging and Sensing Technology Corporation, Horseheads, NY.
- ¹¹Z. Lin, R. L. Boivin, and S. J. Zweben, Princeton Plasma Physics Laboratory Technical Memorandum number PPPL-TM-392, January 1992.
- ¹²M. Tuszewski and S. J. Zweben, *Rev. Sci. Instrum.* **64**, 2459 (1993).
- ¹³A. Ramsey, these proceedings.
- ¹⁴R. L. Boivin, Z. Lin, A. L. Roquemore, and S. J. Zweben, *Rev. Sci. Instrum.* **63**, 4418 (1992).

¹⁵R. J. Hawryluk, et al., Princeton Plasma Physics Laboratory Report number PPPL-2977, to appear in *Phys. Rev. Lett.*

¹⁶J. D. Strachan, et al., Princeton Plasma Physics Laboratory Report number PPPL-2978, to appear in *Phys. Rev. Lett.*

Table 1: Absolute responses of the four probes.

Probe position	R, Absolute response ($\propto \text{cm}^{-2} \text{sec}^{-1}$ (digitizer count / msec) ⁻¹)	Relative response (wrt 90° probe)
90°	2.2×10^7	1.0
60°	9.2×10^7	0.24
45°	4.3×10^7	0.51
20°	5.7×10^7	0.39

Figure Captions

Figure 1: Overview of the layout of the TFTR escaping alpha particle diagnostic, showing the locations of the principal components of the system.

Figure 2: A view of the four escaping alpha particle probes inside the vacuum vessel. Three of the probes are protected from plasma heat flow by the water-cooled graphite disks seen in the photo. The actual probe tips are directly beneath the circular cover at the center of the disks. The fourth probe (at the right) has a cylindrical carbon composite sheath around it.

Figure 3: Each probe contains two apertures which disperse the fusion product ions according to gyroradius and pitch angle onto the scintillator. A 3 μm thick aluminum foil over the slit excludes hydrogenic ions with energies below 300 keV and helium ions with energies below 900 keV.

Figure 4: A diagram of the layout of the optical components in the detector enclosure.

Figure 5: A diagram showing the radiation shielding installed around the fiber optic bundles directly beneath the tokamak.

Figure 6: A plot of the data from the 90° probe, averaged over the interval from 3.4 to 3.7 seconds during shot 73268, showing the camera black level, the background induced by neutrons and gamma rays in the quartz fiber optic bundle, and the signal due to escaping alpha particles.

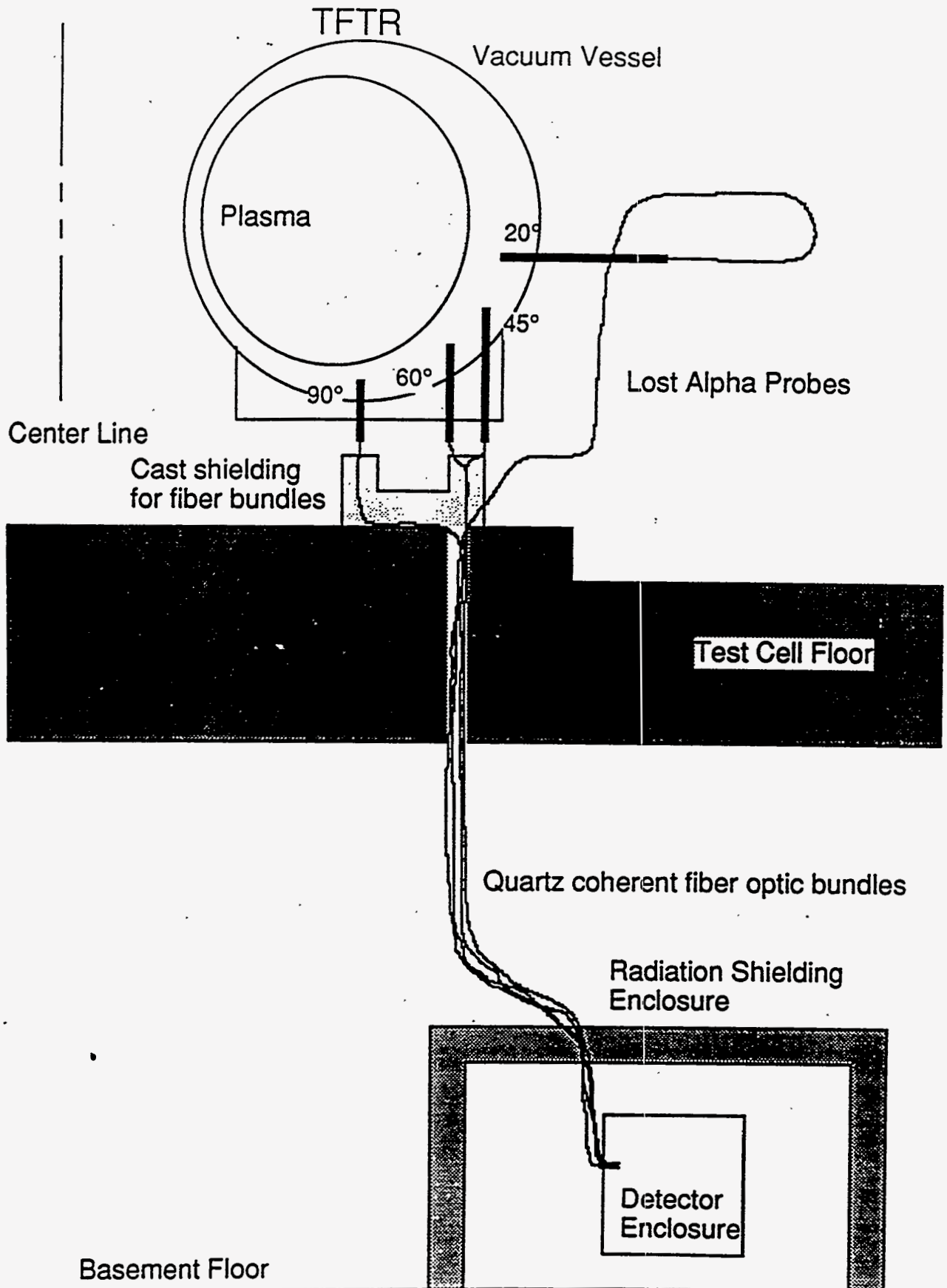


Fig. 1

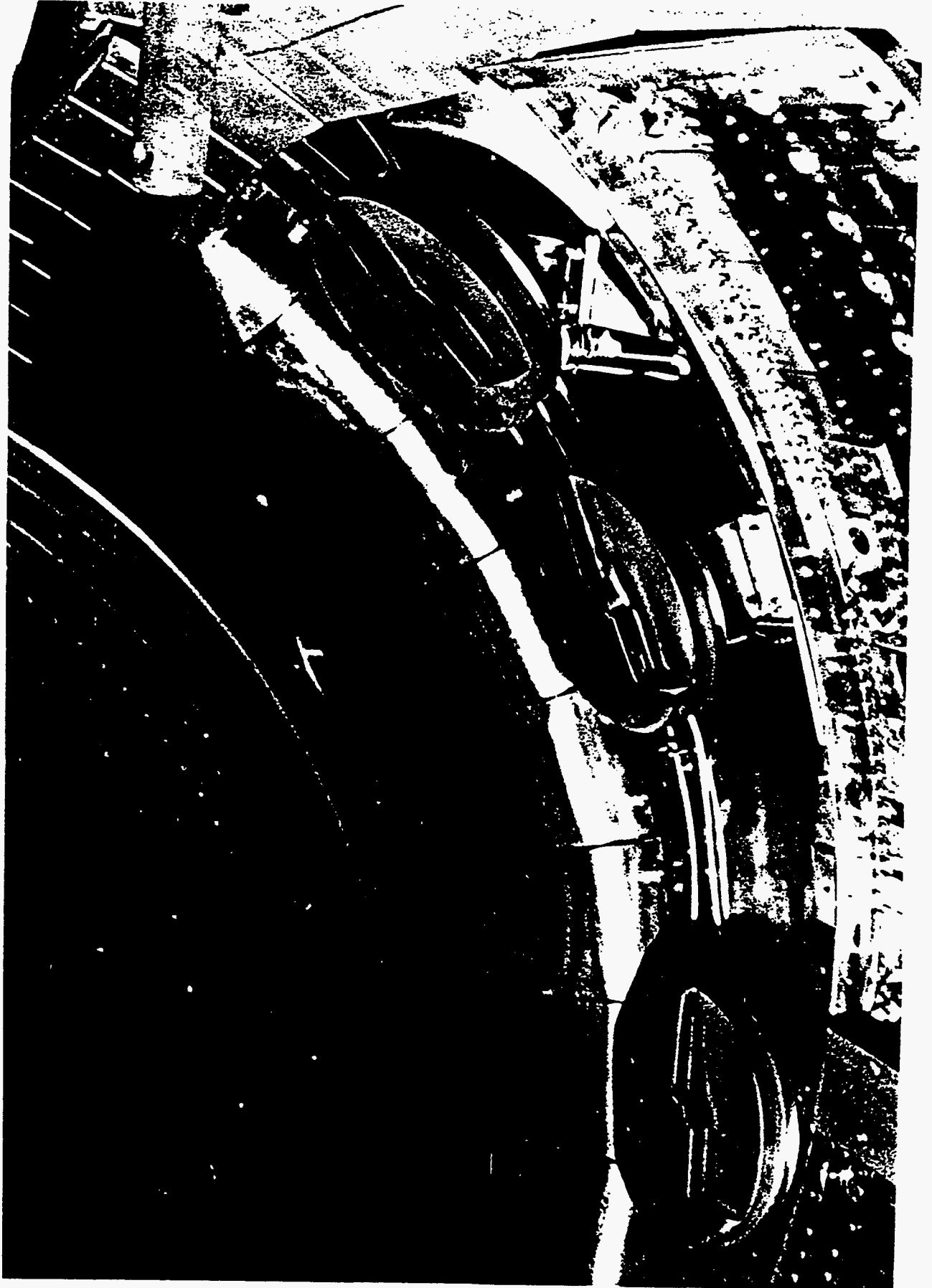


Fig. 2

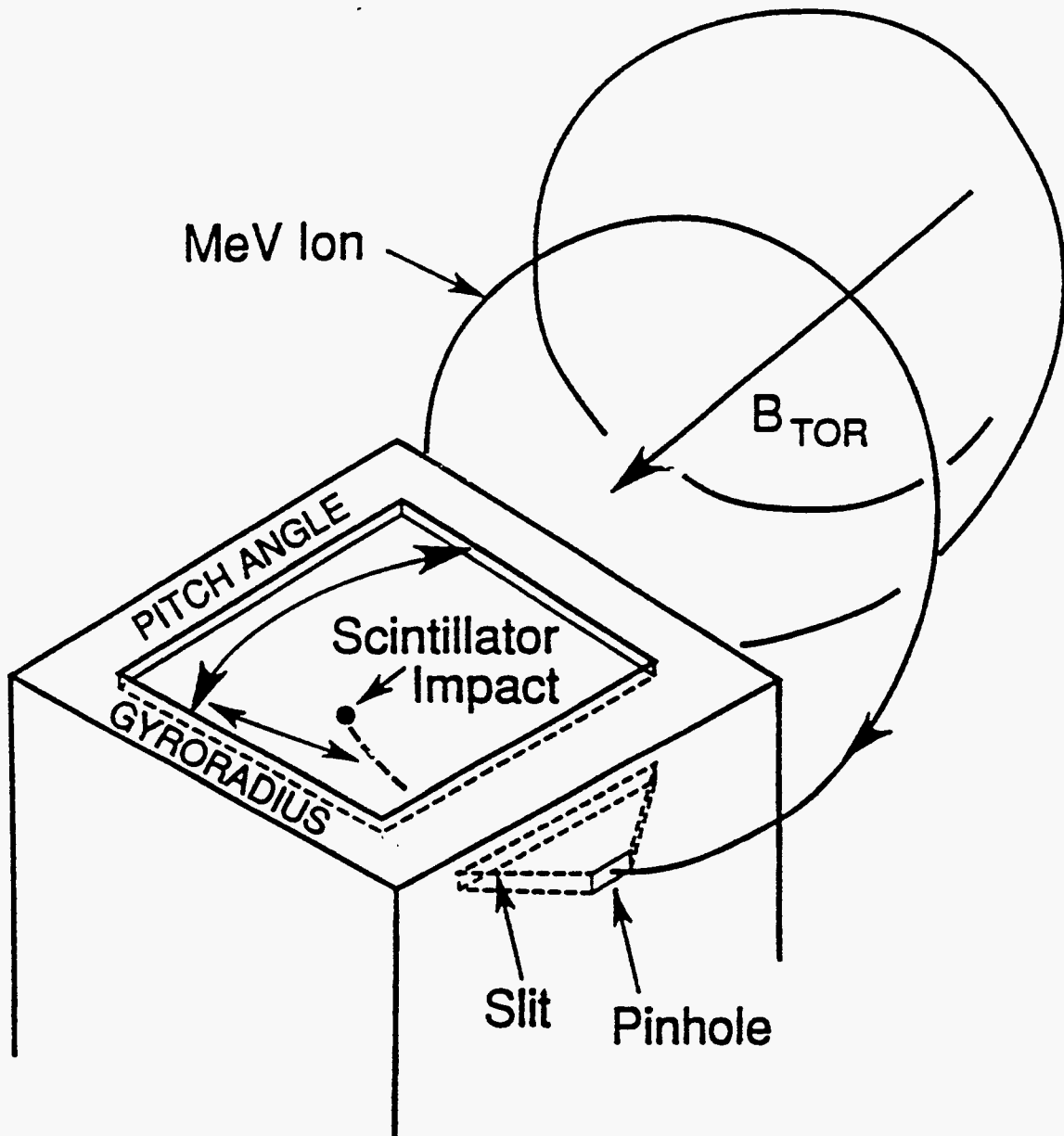


Fig. 3

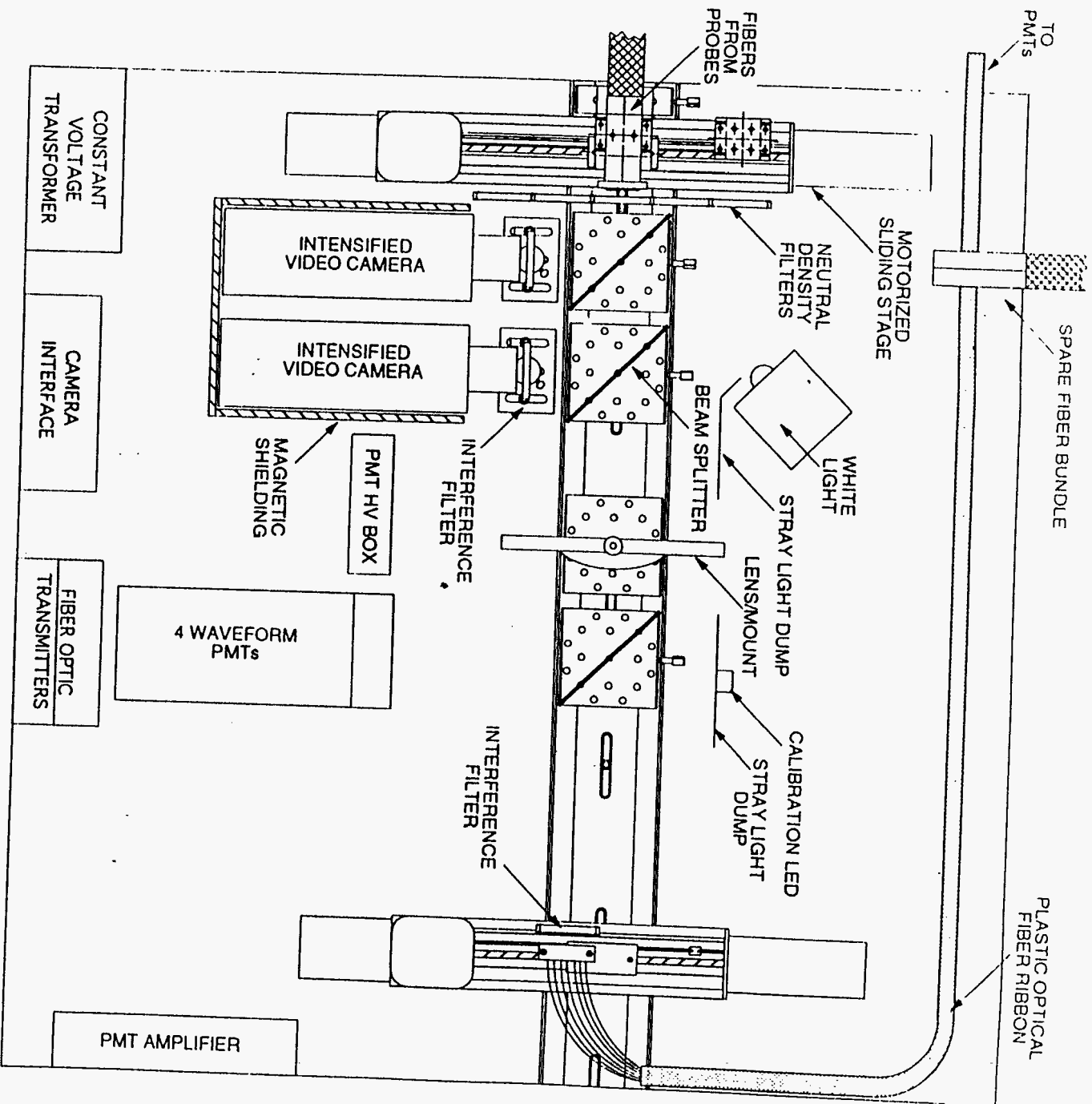
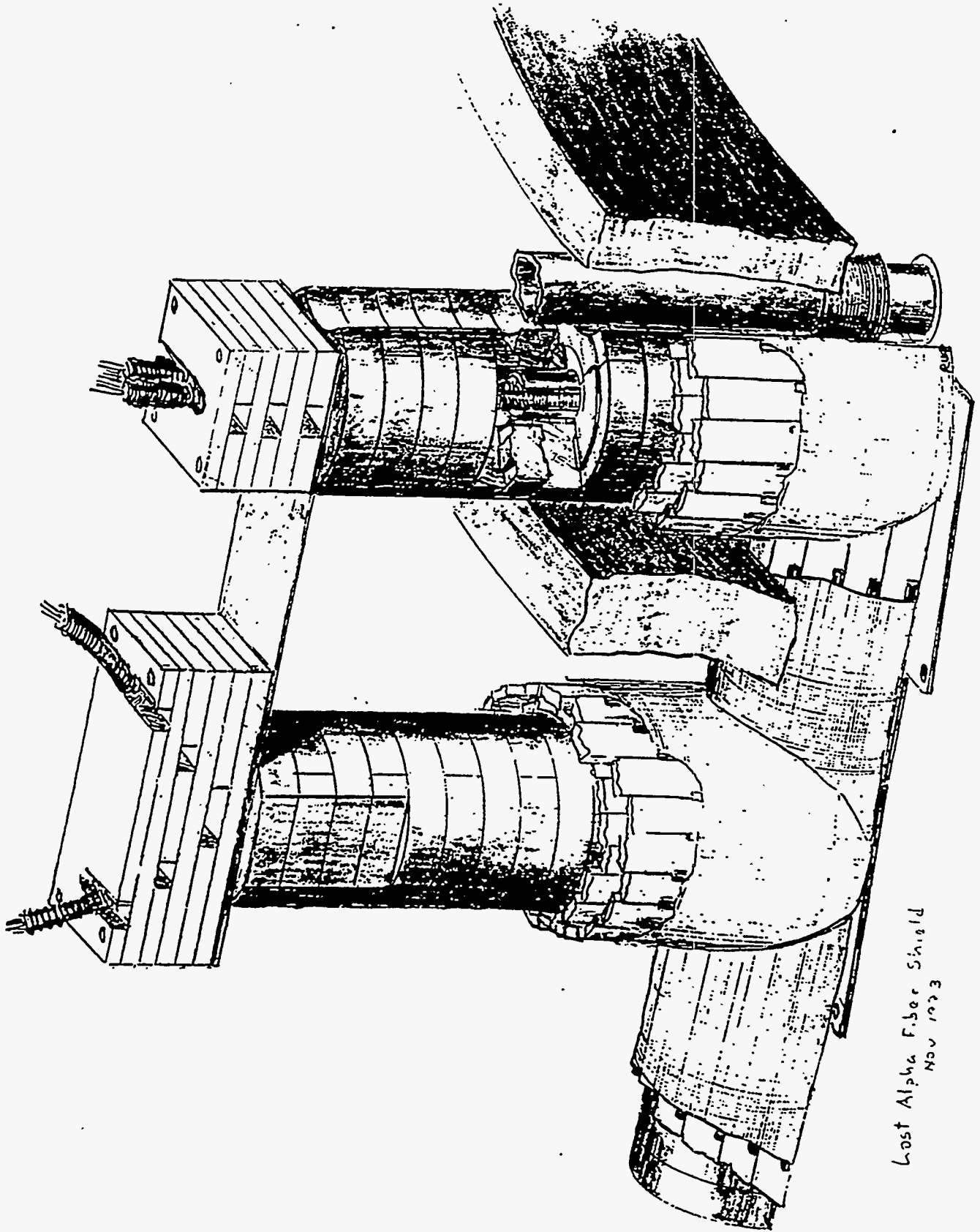


Fig. 4



Lost Alpha Fiber Shield
Nov 1953

Fig. 5

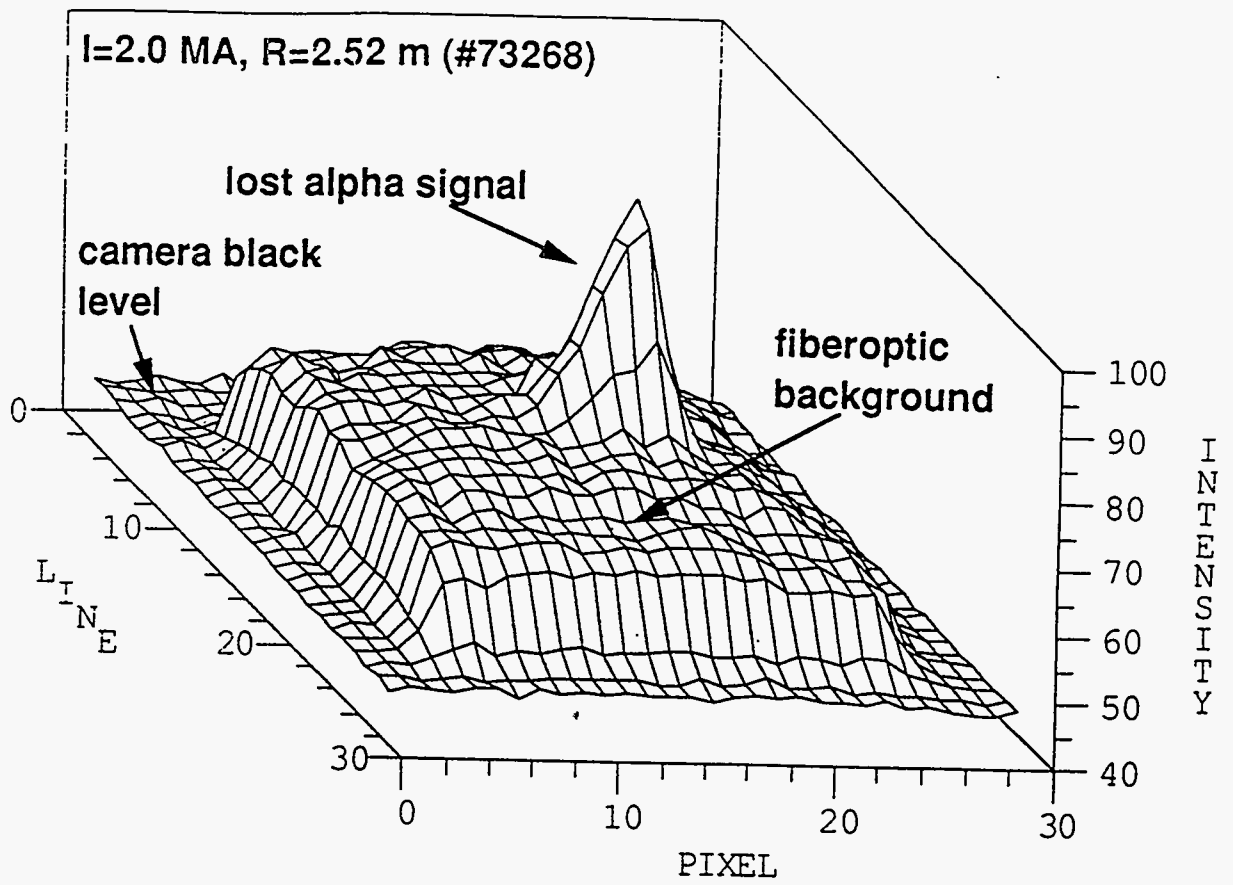


Fig. 6

EXTERNAL DISTRIBUTION IN ADDITION TO UC-420

Dr. F. Paoloni, Univ. of Wollongong, AUSTRALIA
 Prof. R.C. Cross, Univ. of Sydney, AUSTRALIA
 Plasma Research Lab., Australian Nat. Univ., AUSTRALIA
 Prof. I.R. Jones, Flinders Univ, AUSTRALIA
 Prof. F. Cap, Inst. for Theoretical Physics, AUSTRIA
 Prof. M. Heindler, Institut für Theoretische Physik, AUSTRIA
 Prof. M. Goossens, Astronomisch Instituut, BELGIUM
 Ecole Royale Militaire, Lab. de Phy. Plasmas, BELGIUM
 Commission-European, DG. XII-Fusion Prog., BELGIUM
 Prof. R. Bouciqué, Rijksuniversiteit Gent, BELGIUM
 Dr. P.H. Sakanaka, Instituto Fisica, BRAZIL
 Prof. Dr. I.C. Nascimento, Instituto Fisica, Sao Paulo, BRAZIL
 Instituto Nacional De Pesquisas Espaciais-INPE, BRAZIL
 Documents Office, Atomic Energy of Canada Ltd., CANADA
 Ms. M. Morin, CCFM/Tokamak de Varennes, CANADA
 Dr. M.P. Bachynski, MPB Technologies, Inc., CANADA
 Dr. H.M. Skarsgard, Univ. of Saskatchewan, CANADA
 Prof. J. Teichmann, Univ. of Montreal, CANADA
 Prof. S.R. Sreenivasan, Univ. of Calgary, CANADA
 Prof. R. Marchand, INRS-Energie et Materiaux, CANADA
 Dr. R. Bolton, Centre canadien de fusion magnétique, CANADA
 Dr. C.R. James,, Univ. of Alberta, CANADA
 Dr. P. Lukác, Komenského Univerzita, CZECHO-SLOVAKIA
 The Librarian, Culham Laboratory, ENGLAND
 Library, R61, Rutherford Appleton Laboratory, ENGLAND
 Mrs. S.A. Hutchinson, JET Library, ENGLAND
 Dr. S.C. Sharma, Univ. of South Pacific, FIJI ISLANDS
 P. Mähönen, Univ. of Helsinki, FINLAND
 Prof. M.N. Bussac, Ecole Polytechnique,, FRANCE
 C. Mouttet, Lab. de Physique des Milieux Ionisés, FRANCE
 J. Radet, CEN/CADARACHE - Bat 506, FRANCE
 Prof. E. Economou, Univ. of Crete, GREECE
 Ms. C. Rinni, Univ. of Ioannina, GREECE
 Preprint Library, Hungarian Academy of Sci., HUNGARY
 Dr. B. DasGupta, Saha Inst. of Nuclear Physics, INDIA
 Dr. P. Kaw, Inst. for Plasma Research, INDIA
 Dr. P. Rosenau, Israel Inst. of Technology, ISRAEL
 Librarian, International Center for Theo Physics, ITALY
 Miss C. De Palo, Associazione EURATOM-ENEA , ITALY
 Dr. G. Grosso, Istituto di Fisica del Plasma, ITALY
 Prof. G. Rostangni, Istituto Gas Ionizzati Del Cnr, ITALY
 Dr. H. Yamato, Toshiba Res & Devel Center, JAPAN
 Prof. I. Kawakami, Hiroshima Univ., JAPAN
 Prof. K. Nishikawa, Hiroshima Univ., JAPAN
 Librarian, Naka Fusion Research Establishment, JAERI, JAPAN
 Director, Japan Atomic Energy Research Inst., JAPAN
 Prof. S. Itoh, Kyushu Univ., JAPAN
 Research Info. Ctr., National Instit. for Fusion Science, JAPAN
 Prof. S. Tanaka, Kyoto Univ., JAPAN
 Library, Kyoto Univ., JAPAN
 Prof. N. Inoue, Univ. of Tokyo, JAPAN
 Secretary, Plasma Section, Electrotechnical Lab., JAPAN
 Dr. O. Mitarai, Kumamoto Inst. of Technology, JAPAN
 Dr. G.S. Lee, Korea Basic Sci. Ctr., KOREA
 J. Hyeon-Sook, Korea Atomic Energy Research Inst., KOREA
 D.I. Choi, The Korea Adv. Inst. of Sci. & Tech., KOREA
 Prof. B.S. Liley, Univ. of Waikato, NEW ZEALAND
 Inst of Physics, Chinese Acad Sci PEOPLE'S REP. OF CHINA
 Library, Inst. of Plasma Physics, PEOPLE'S REP. OF CHINA
 Tsinghua Univ. Library, PEOPLE'S REPUBLIC OF CHINA
 Z. Li, S.W. Inst Physics, PEOPLE'S REPUBLIC OF CHINA
 Prof. J.A.C. Cabral, Instituto Superior Tecnico, PORTUGAL
 Prof. M.A. Hellberg, Univ. of Natal, S. AFRICA
 Prof. D.E. Kim, Pohang Inst. of Sci. & Tech., SO. KOREA
 Prof. C.I.E.M.A.T, Fusion Division Library, SPAIN
 Dr. L. Stenflo, Univ. of UMEA, SWEDEN
 Library, Royal Inst. of Technology, SWEDEN
 Prof. H. Wilhelmson, Chalmers Univ. of Tech., SWEDEN
 Centre Phys. Des Plasmas, Ecole Polytech, SWITZERLAND
 Bibliotheek, Inst. Voor Plasma-Fysica, THE NETHERLANDS
 Asst. Prof. Dr. S. Cakir, Middle East Tech. Univ., TURKEY
 Dr. V.A. Glukhikh, Sci. Res. Inst. Electrophys.I Apparatus, USSR
 Dr. D.D. Ryutov, Siberian Branch of Academy of Sci., USSR
 Dr. G.A. Eliseev, I.V. Kurchatov Inst., USSR
 Librarian, The Ukr.SSR Academy of Sciences, USSR
 Dr. L.M. Kovrizhnykh, Inst. of General Physics, USSR
 Kernforschungsanlage GmbH, Zentralbibliothek, W. GERMANY
 Bibliothek, Inst. Für Plasmaforschung, W. GERMANY
 Prof. K. Schindler, Ruhr-Universität Bochum, W. GERMANY
 Dr. F. Wagner, (ASDEX), Max-Planck-Institut, W. GERMANY
 Librarian, Max-Planck-Institut, W. GERMANY